

# Metal Additive Micro-Manufacturing to Achieve Enhanced Air-Bridge Geometry for Coplanar Waveguide mm-Wave GaN-on-SiC Integrated Circuits

Arthur Collier<sup>1</sup>, Abdalla Eblabla<sup>1</sup>, Wesley Sampson<sup>1</sup>, Elham Yadollahifarsi<sup>1</sup>, Edgar Hepp<sup>2</sup>, Ricardo Conte<sup>2</sup>, Khaled Elgaid<sup>1</sup>

<sup>1</sup>Centre for High Frequency Engineering, Cardiff University, CF24 3AA, UK ([colliera2@cardiff.ac.uk](mailto:colliera2@cardiff.ac.uk), +442920874000)

<sup>2</sup>Exaddon AG, 8152 Glattbrugg, Switzerland ([hello@exaddon.com](mailto:hello@exaddon.com), +41445204545)

**Keywords:** coplanar waveguides, interconnects, mm-wave, sub-THz, MMIC applications, metal 3D printing

## Abstract

**This paper presents a novel cavity coplanar waveguide (CCPW) structure based on GaN-on-SiC technology for high-power microwave applications. The CCPW structure was fabricated using an emerging monolithic microwave integrated circuit (MMIC)-compatible localised electrodeposition metal additive micro-manufacturing ( $\mu$ AM) process, achieving an air-bridge height of 50  $\mu$ m. Electromagnetic (EM) simulations revealed that introducing a cavity above the CPW improves impedance matching at mm-wave frequencies while providing a robust ground-return path. S-parameter measurements show that the CCPW provides a 6.5 dB improvement in reflection coefficient at 110 GHz compared to a standard coplanar waveguide (CPW) structure. Furthermore, both simulations and measurements indicate a broadband reflection coefficient trough suggesting the potential for broadband impedance matching in MMIC applications. To further analyse RF parasitics, a high-frequency equivalent circuit model was developed, demonstrating significant performance improvements of the CCPW compared to a printed air-bridge.**

## INTRODUCTION

Applications for monolithic microwave integrated circuits (MMIC) operating at mm-wave frequencies are growing in demand, ranging from high-data-rate communications for 5G/6G mobile networks and backhaul communications [1] to imaging, spectroscopy, and automotive radar [2]. GaN-on-SiC has been utilised to demonstrate state-of-the-art V-band (50 - 75 GHz) and W-band (75 - 110 GHz) integrated circuits [2], [3]. As operating frequencies increase, high-quality impedance matching between MMIC components is fundamental to optimise power transfer and maximise efficiency.

Coplanar waveguide (CPW) interconnect technology offers advantages for mm-wave MMICs by eliminating the need for complex backside processing [4]. Air-bridges are imperative for CPW-based MMICs for signal routing and coupled-slotline mode suppression at impedance discontinuities. However, air-bridges contribute parasitic

effects due to the proximity of the bridge to signal paths below. Standard air-bridge fabrication processes utilise a resist or dielectric as temporary support, constraining fabrication geometry. Air-bridges for high-quality MMIC passives have been reported at heights around 5  $\mu$ m [5], while industrial processes are typically in the 1 - 2  $\mu$ m range for high yield processes at wafer level.

Emerging fabrication methods, such as localised electrodeposition metal additive micro-manufacturing ( $\mu$ AM), have enabled 3-D, highly conductive structures with sub-micron features. The potential of this method for mm-wave integrated circuits is gathering research attention, with demonstrations including a mm-wave helical travelling-wave tube [6].

This work demonstrates the integration of  $\mu$ AM into the GaN-on-SiC MMIC fabrication process to extend beyond the height constraints of standard air-bridge technology, with fabricated devices spanning 50  $\mu$ m above the CPW. The concept of a cavity coplanar waveguide (CCPW) is demonstrated and shown to exhibit enhanced matching compared to a bare CPW while providing an essential CPW ground-to-ground connection. A high-frequency open-circuited equivalent circuit model was derived to quantify parasitic effects of the developed CCPW, showing reduced parasitic series resistance and capacitance, while maintaining negligible shunt capacitance due to the height of the cavity.

## SIMULATION

A full-wave electromagnetic simulator was used to quantify the influence of the CCPW height on reflection and transmission coefficients. A 200  $\mu$ m long, 50  $\Omega$  CPW (33  $\mu$ m width, 20  $\mu$ m gap, 0.35  $\mu$ m thick Au) was positioned on a 500  $\mu$ m thick SiC substrate. For the cavity, two Cu supports with 150  $\mu$ m length and 9  $\mu$ m width were placed at the waveguide midpoint on each ground plane. The bridge supports were connected with a 168  $\mu$ m Cu span object to form a 150  $\mu$ m gap between supports. A discrete S-parameter simulation was conducted up to 110 GHz with cavity heights ranging from 5  $\mu$ m to 50  $\mu$ m. Fig. 1 illustrates how increasing the cavity height improved both transmission and reflection coefficients for CCPWs, particularly at W-band frequencies, while heights

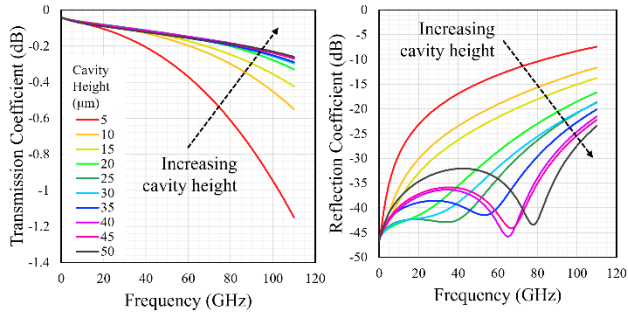


Fig. 1. Simulated S-parameters of CCPWs with various heights above the CPW (a) transmission coefficient (b) reflection coefficient.

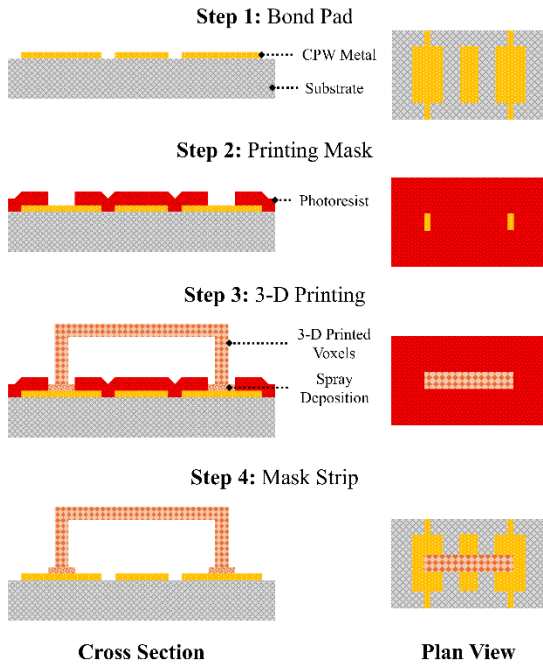


Fig. 2. Cross-sectional and plan view diagrams of air-bridge and cavity fabrication process (not to scale).

achievable by conventional fabrication methods were not effective. Furthermore, for taller structures a peak match occurs and could be engineered for matching the desired frequency by controlling the height of the cavity.

FABRICATION

Devices were fabricated using 6-inch GaN-on-SiC with a substrate thickness of 500  $\mu\text{m}$ . Air-bridges (50  $\mu\text{m}$  long) and cavities (150  $\mu\text{m}$  long), which were defined as an extended air-bridge that encapsulated most of the transmission line, were fabricated using the process outlined by Fig. 2. Mask-less lithography and electron-beam metal evaporation were used to fabricate the Ti/Au (50/300) nm thick CPW lines. A second lithography step defined a protective photoresist print mask to expose the bridge support print locations, preventing

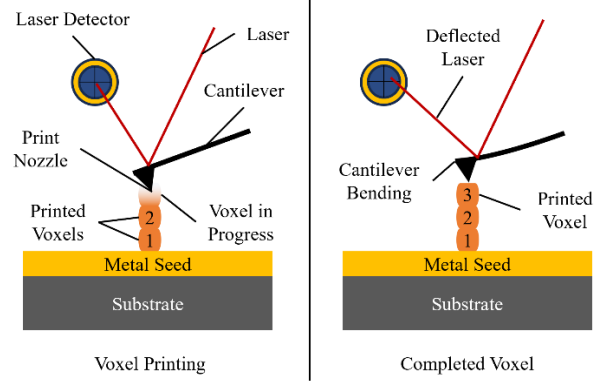


Fig. 3. CERES  $\mu\text{AM}$  voxel printing process control through deflection of laser on cantilever.

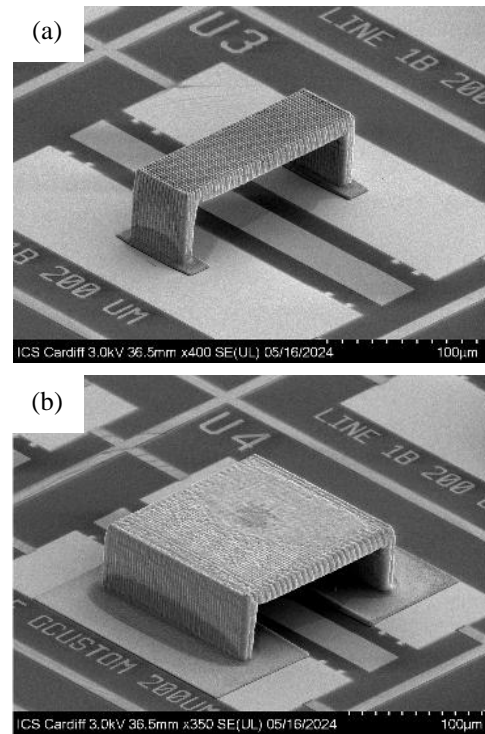


Fig. 4. SEM of CPWs with printed 3-D structure (a) air-bridge (b) cavity.

unwanted Cu deposition on surrounding areas of the sample from ink spray. The sample was then loaded into the Exaddon CERES  $\mu\text{AM}$  system, which achieves high precision localised electrodeposition of highly conductive 3-D structures. The sample was immersed in the printing chamber by an electrolyte where Cu ions were delivered to the point of deposition through a cantilever tip with a microfluidic channel. The completion of a voxel is detected by laser deflection from the cantilever bending upwards, as illustrated by Fig. 3. A 300 nm iontip was used with Cu iontip ink with standard brightener ratios, as specified by the tool manufacturer. Cu air-bridges and cavities with a height of 50  $\mu\text{m}$  were printed onto CPWs with spatial parameters matching

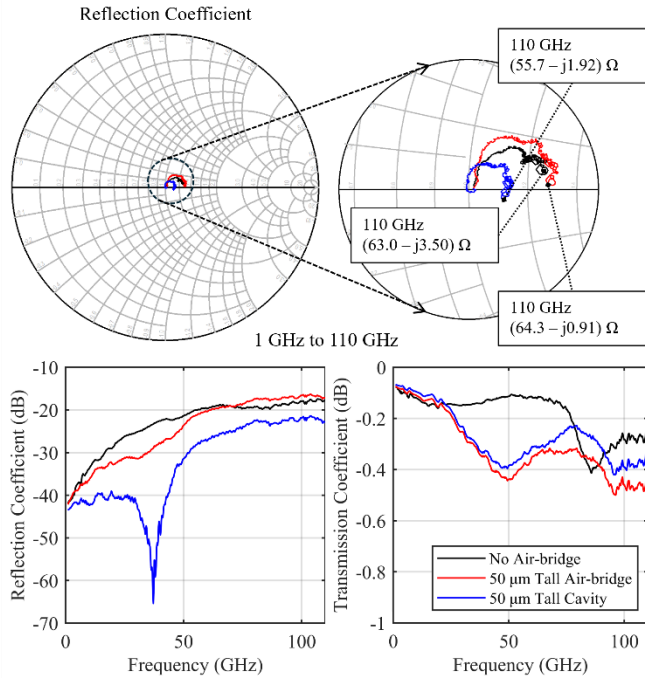


Fig. 5. Measured 2-port S-parameters of a bare CPW with no bridge, a CPW with a 50  $\mu\text{m}$  tall air-bridge, and a CPW with a 50  $\mu\text{m}$  tall cavity.

the simulation model. Voxels had a pitch of 3  $\mu\text{m}$ , a height of 1  $\mu\text{m}$ , and were printed at 100 mBar. Multiple bridges were printed sequentially using a single alignment step; in this work, air-bridges and cavities were printed across a 1-inch<sup>2</sup> area in succession. After completion of printing, the resist mask was stripped. Fig. 4 illustrates the successful implementation of an air-bridge and a cavity aligned centrally to pre-existing CPW structures on the GaN-on-SiC substrate.

#### SMALL SIGNAL CHARACTERISATION

S-parameter measurements were performed using a vector network analyser (Keysight N5227B) with a 110 GHz frequency extender (Keysight N5293AX03). Ground-signal-ground probes with a pitch of 100  $\mu\text{m}$  and a maximum operating frequency of 110 GHz (MPI T110A GSG100) were calibrated up to 110 GHz using multi-line thru-reflect-line calibration protocol on a standard calibration substrate.

Fig. 5 demonstrates that extending an air-bridge into a cavity structure results in improved reflection and transmission coefficients at all measured frequencies. Comparing the high frequency performance of a bare CPW to the CCPW shows reflection coefficients at 110 GHz of -18.5 dB and -25.0 dB, respectively, indicating a 35% improvement without compromising insertion loss, remaining below -0.4 dB. Furthermore, the wide-bandwidth trough in reflection coefficient that was predicted by simulations was present in the measurements, representing the potential to target matching over a specified bandwidth. While the matching

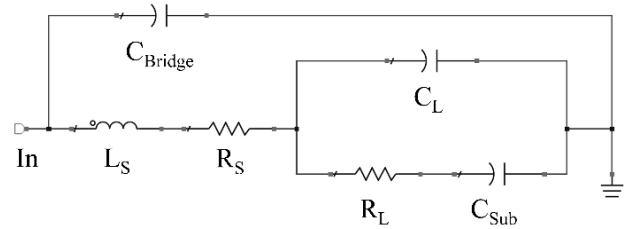


Fig. 6. Equivalent circuit model for both CPW with printed air-bridge and CPW with printed cavity.

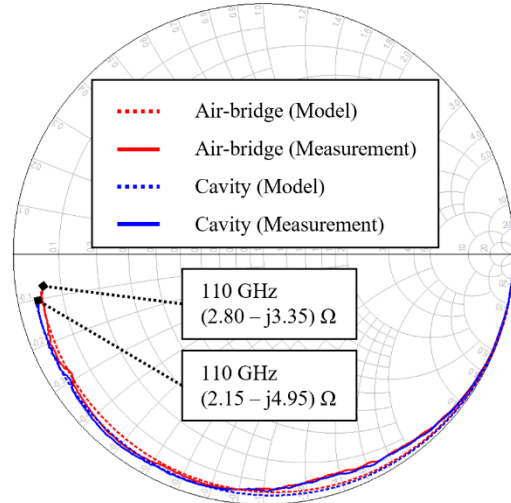


Fig. 7. Reflection coefficient Smith chart of both modelled and measured data for CPW with airbridge and CPW with cavity.

peak shifted in frequency between simulation and measurement, one could infer that predictions of frequency could be refined through simulation, fabrication, and measurement of a wider range of cavity pitch, height, and length.

#### EQUIVALENT CIRCUIT MODELLING

An open-circuited CPW line equivalent circuit model considering the air-bridge/cavity effect was developed for both the CPW with an air-bridge and the CCPW up to 110 GHz, as shown in Fig. 6.  $R_S$  as  $L_S$  represents the signal line metal parasitics, while  $R_L$ ,  $C_L$  and  $C_{Sub}$  represent the signal line-to-ground of the CPW including substrate coupling effects. The shunt capacitance,  $C_{Bridge}$  represents the ground-connected bridge.

Fig. 7 depicts one-port measurements of both air-bridge and cavity structures and the fitted equivalent circuit model for both devices. The lumped element equivalent circuit model fits well for both devices across the W-band. However, deviation at frequencies below the W-band may be due to system calibration limitations and the model being optimised specifically for W-band operation. The impedance at higher

frequencies indicates that the CCPW is a more efficient transmission medium than the CPW with air-bridge. The lumped element parameters were extracted and tabulated by Table 1. Compared to the air-bridge device, the CCPW exhibited a 26% reduction in  $C_L$  and a 27% reduction in  $R_S$ . Other circuit parameters were unaffected by differences between devices, including  $C_{Bridge}$ ; due to the height of the cavity, the additional parallel plate area presented by the length of the cavity induced negligible parasitic capacitance.

TABLE I

EXTRACTED LUMPED ELEMENT PARAMETERS FROM AIR-BRIDGE AND CAVITY S-PARAMETERS.

Circuit Element	CPW with 50 $\mu\text{m}$ air-bridge	CPW with 50 $\mu\text{m}$ cavity
$L_S$ (fH)	16.2	16.2
$R_S$ ( $\Omega$ )	2.6	1.9
$C_L$ (fF)	354	262
$R_L$ (k $\Omega$ )	876	876
$C_{Sub}$ (fF)	60	60
$C_{Bridge}$ (fF)	2.1	2.1

## CONCLUSIONS

This work demonstrated the successful integration of  $\mu\text{AM}$  fabrication methods into the GaN MMIC process flow, enabling enhanced air-bridge geometries outside the constraints of conventional methods. The novel CCPW structure was simulated and fabricated, with S-parameter measurements indicating enhanced matching at V-band and W-band frequencies while also providing a vital ground-to-ground connection for the suppression of parasitic modes in CPWs. Measurements confirmed that the CCPW had enhanced matching and reduced insertion loss compared to the printed air-bridge on a CPW, while modelling illustrated mitigation of RF parasitics, achieving a 26% and 27% reduction in  $C_L$  and  $R_S$ , respectively. These findings highlight the viability of CCPW technology for broadband impedance matching and its promising application in high power mm-wave and sub-THz MMICs, advancing future high-frequency electronics.

## ACKNOWLEDGEMENTS

The authors would like to acknowledge the Engineering and Physical Sciences Research Council (EPSRC) for funding our research activity.

## REFERENCES

- [1] F. Medjdoub *et al.*, "Emerging GaN Technologies for Next-Generation Millimeter-Wave Applications," in *IEEE Microwave Magazine*, vol. 25, no. 10, pp. 18-37, Oct. 2024, doi: 10.1109/MMM.2024.3428188.
- [2] T. Sonnenberg, *et al.*, "V- and W-Band Millimeter-Wave GaN MMICs," in *IEEE Journal of Microwaves*, vol. 3, no. 1, pp. 453-465, Jan. 2023, doi: 10.1109/JMW.2022.3221281.
- [3] T. Sonnenberg, *et al.*, "A W-Band GaN MMIC Single-Chip T/R Front End," in *IEEE Transactions on Microwave Theory and Techniques*, vol. 72, no. 10, pp. 5830-5837, Oct. 2024, doi: 10.1109/TMTT.2024.3422156.
- [4] S. Piotrowicz *et al.*, "43 W, 52% PAE X-Band AlGaIn/GaN HEMTs MMIC amplifiers", *2010 IEEE MTT-S International Microwave Symposium*, Anaheim, CA, USA, Jun. 2010, pp. 505-508, doi: 10.1109/MWSYM.2010.5518097.
- [5] A. Eblabla, *et al.*, "Low-Loss MIM Capacitor on Thick SiO<sub>2</sub> Dielectric for GaN-on-Si Substrates with Standard and Elevated Top Electrode Configurations", *2023 53rd European Microwave Conference (EuMC)*, Berlin, Germany, Sep. 2023, pp. 38-41, Sep 2023, doi: 10.23919/EuMC58039.2023.10290587.
- [6] G. Ulisse, *et al.*, "A 3-D Printed Helix for Traveling-Wave Tubes," in *IEEE Transactions on Electron Devices*, vol. 69, no. 11, pp. 6358-6361, Nov. 2022, doi: 10.1109/TED.2022.3209645.

## ACRONYMS

CCPW: Cavity Coplanar Waveguide  
 MMIC: Monolithic Microwave Integrated Circuit  
 $\mu\text{AM}$ : Metal Additive Micro-manufacturing  
 EM: Electromagnetic  
 CPW: Coplanar Waveguide